GlcNAcstatins are nanomolar inhibitors of human O-GlcNAcase inducing cellular hyper-O-GlcNAcylation

Helge C Dorfmueller, Vladimir S Borodkin, Marianne Schimpl, Daan Mf van Aalten

GlcNAcstatins are nanomolar inhibitors of human *O*-GlcNAcase inducing cellular hyper-*O*-GlcNAcylation

Helge C. Dorfmueller, Vladimir S. Borodkin, Marianne Schimpl and Daan M.F. van Aalten*

Division of Molecular Microbiology, College of Life Sciences, University of Dundee, Dundee DD1 5EH, Scotland.

* To whom correspondence should be addressed.

E-mail: dava@davapc1.bioch.dundee.ac.uk, Fax: ++ 44 1382 345764

Abstract

***O*-GlcNAcylation is an essential, dynamic and inducible posttranslational glycosylation of cytosolic proteins in metazoa and can show interplay with protein phosphorylation. Inhibition of *O*-GlcNAcase (OGA), the enzyme that removes *O*-GlcNAc from *O*-GlcNAcylated proteins, is a useful strategy to probe the role of this modification in a range of cellular processes. Here, we report the rational design and evaluation of GlcNAcstatins, a family of potent, competitive and selective inhibitors of human OGA. Kinetic experiments with recombinant human OGA reveal that the GlcNAcstatins are the most potent human OGA inhibitors reported to date, inhibiting the enzyme in the sub-nanomolar to nanomolar range. Modification of the GlcNAcstatin *N*-acetyl group leads to up to 160-fold selectivity against the human lysosomal hexosaminidases which employ a similar substrate-assisted catalytic mechanism. Mutagenesis studies in a bacterial OGA, guided by the structure of a GlcNAcstatin complex, provides insight into the role of conserved residues in the human OGA active site. GlcNAcstatins are cell-permeable and, at low nanomolar concentrations, effectively modulate intracellular *O*-GlcNAc levels through inhibition of OGA, in a range of human cell lines. Thus, these compounds are potent, selective tools to study the cell biology of *O*-GlcNAc.**

Introduction

Reversible posttranslational modification of many cytoplasmic and nuclear proteins in eukaryotic cells by glycosylation of serine and threonine residues with β-linked *N*-acetylglucosamine (*O*-GlcNAc) has been shown to play important roles in cellular processes as diverse as DNA transcription and translation, insulin sensitivity, protein trafficking and degradation [1, 2, 3, 4]. Dysregulation of *O*-GlcNAc appears to play a role in human pathogenesis, such as cancer [5, 6, 7] and Alzheimer's [8, 9, 10, 11, 12]. *O*-GlcNAc is also implicated in diabetes type II [13, 14], however, the precise mechanism is still controversial [15].

In higher eukaryotes only two enzymes are responsible for the dynamic cycling of *O*-GlcNAc, the *O*-GlcNAc transferase (OGT, CAZY family GT41 [16]) that transfers GlcNAc onto proteins from the UDP-GlcNAc donor, and the *O*-GlcNAcase, that catalyzes the removal of *O*-GlcNAc (OGA, GH84 [17]). The precise molecular mechanisms by which OGT and OGA recognise and act on hundreds of proteins remain to be discovered [18].

Inhibition of human OGA (hOGA) with *O*-(2-acetamido-2-deoxy-D-glucopyranosylidene)amino *N*-phenylcarbamate (PUGNAc, Fig. 1A) (K_i = 50 nM [19, 20]) has been used extensively to study the role of *O*-GlcNAc in a range of cellular processes [21, 22, 23, 24, 25, 26, 27]. Crystal structures of bacterial hOGA homologues have recently become available [28, 29], and it has been shown that PUGNAc is a tight-binding inhibitor, with its imidolactone ring mimicking the half-chair/envelope conformation of the pyranose ring in the transition state by virtue of the stable oxime moiety [28, 30]. However, PUGNAc also potently inhibits the human hexosaminidases A/B (HexA/B; GH20), genetic inactivation of which has been associated with the Tay-Sachs and Sandhoff lysosomal storage disorders [31]. Structural analysis has revealed that the acetamido group of PUGNAc resides in a deep pocket that is significantly larger in OGAs than in the lysosomal hexosaminidases HexA/HexB [32, 28, 29]. The feasibility of constructing more selective PUGNAc analogues, as well as other hOGA inhibitors that exploit the difference in the size of the *N*-acyl binding pocket, has recently been explored [20, 33, 34]. Increasing the size of the *N*-acyl substituents, however, also resulted in weaker (micromolar) inhibition of hOGA. Furthermore, PUGNAc is acid labile [35]. Thiazoline, another inhibitor of GH20/84 enzymes [32, 36, 37], has also been similarly chemically modified to achieve more

selective *O*-GlcNAcase inhibition, yielding derivatives that inhibited in the low μM range with three orders of magnitude selectivity towards hOGA [20, 33], culminating in the recent report of the thiazoline derivative thiamet-G, with selectivity towards hOGA, inhibiting it with a K_i of 21 nM [38].

We have recently reported a novel scaffold, GlcNAcstatin, a potent inhibitor of a bacterial OGA orthologue, exploiting the structural similarity of *Z*-PUGNAc and the naturally occurring potent hexosaminidase inhibitor nagstatin (Fig. 1A) [39, 40, 41]. Inhibition of β-glycosidases with nagstatin-related sugar-imidazoles have been examined by Vasella *et al.*, who suggested that lateral protonation of the exo-cyclic nitrogen atom of the imidazole ring should account for the excellent inhibiting properties of these compounds [42]. Indeed, GlcNAcstatin inhibited a bacterial OGA orthologue in the picomolar range, and structural analysis revealed a tight interaction between the catalytic acid and the (presumbly protonated) imidazole [41].

Here, we report that GlcNAcstatin also potently inhibits hOGA, with a K_i in the low nanomolar range. We also show that this compound is able to induce hyper-*O*-GlcNAcylation in a range of human cell lines when used at low nanomolar concentrations. Furthermore, we report four new GlcNAcstatin derivatives that explore potency and selectivity of this scaffold, with one of these being the most potent hOGA inhibitor reported so far, inhibiting with a K_i of 420 pM. Guided by a crystal structure of one of these derivatives in complex with a bacterial OGA, we probe key interactions through mutagenesis. These novel molecules will be useful tools for the study of *O*-GlcNAc in a range of cellular signal transduction pathways.

Materials and methods

Cloning, protein expression and purification

The previously described plasmid for expression of the OGA orthologue from *Clostridium perfringens* (*Cp*OGA) [28] was used as a template to carry out mutagenesis of Val331 to cysteine, using QuikChange kit (Stratagene) with the following primers: 5'-GGGAGATGTAAAACCATTAATAACATGCCCAACAGAGTATGATACTGGAGC-3' and 5'-GCTCCAGTATCATACTCTGTTGGGCATGTTATTAATGGTTTTACATCTCCC-3'. Trp490Ala mutagenesis was performed using the same protocol and techniques with primers: 5'-GGACAATAAAACTGCGGCTAAATCAGGAAG-3' and 5'-CTTCCTGATTTAGCCGCAGTTTTATTGTCC-3'. The constructs were verified by DNA-sequencing. V331C-*Cp*OGA, W490A-*Cp*OGA and wild type protein were expressed and purified following the protocol described previously [28, 41, 43].

hOGA (53-916) was cloned into a modified version of pGEX6P-1, lacking the *Bam*HI site, and the human OGA sequence was inserted using *Eco*RI and *Not*I sites, after an internal *Eco*RI site was removed by introducing a silent mutation. The protein was expressed in *E. coli* BL21 (DE3) cells overnight at 15 °C using 10 μM IPTG (OD_{600} of 0.4-0.6). The cells were harvested by centrifugation and lysed with sonication in lysis buffer (50 mM Tris/HCl pH 7.5, 250 mM NaCl, 1 mM EDTA, 1 mM EGTA, 0.1% β-mercaptoethanol, 0.2 mM PMSF, 1 mM benzamidine). The recombinant GST-fusion protein was bound to glutathione sepharose beads that were pre-equilibrated in washing buffer (50 mM Tris/HCl pH 7.5, 250 mM NaCl, 1 mM EGTA, 0.1% β-mercaptoethanol, 0.2 mM PMSF, 1 mM benzamidine). The fusion protein was eluted using the washing buffer supplemented with 20 mM glutathione and pH adjusted to 7.5. The eluted protein was dialysed into 50 mM Tris/HCl pH 7.5, 0.1 mM EGTA, 150 mM NaCl, 0.07% β-mercaptoethanol, 0.1 mM PMSF, 1 mM benzamidine.

Determination of the CpOGA-GlcNAcstatin D complex structure

*Cp*OGA was crystallised as described previously [28, 41, 43]. 1 μl of a suspension of GlcNAcstatin D in mother liquor was added to the crystallised protein in a 2.25 μl drop (1 μl protein plus 1 μl

mother liquor plus 0.25 μl 40 % γ-butyrolactone). After 50 min at 20 °C (RT) the crystal was cryoprotected by 5 s immersion in 0.17 M ammonium sulfate, 0.085 M sodium cacodylate, pH 6.5, 25.5% PEG 8000 and 15% glycerol and frozen in a nitrogen cryostream. Data were collected at the European Synchrotron Radiation Facility on beamline ID14-1 to 2.3 Å, with an overall R_{merge} of 0.074 and 98.2% completeness. Refinement was initiated from the native *Cp*OGA-GlcNAcstatin C complex (PDB entry 2J62, [41]). Well-defined F_o-F_c electron density for the inhibitor was observed (Fig. 2A), allowing placement of an inhibitor model, built with the help of a PRODRG [44] structure and topology. Iterative model building using COOT [45] and refinement with REFMAC [46] yielded the final model with good statistics (R, R_{free}: 18.5, 23.8).

Inhibition measurements

Steady-state kinetics of wild type hOGA and *Cp*OGA mutants were determined using the fluorogenic substrate 4-methylumbelliferyl-*N*-acetyl-β-D-glucosaminide (4MU-NAG; Sigma). Standard reaction mixtures (50 μl) contained 2 pM *Cp*OGA mutant in 50 mM citric acid, 125 mM Na_2HPO_4 (pH 5.5), 0.1 mg/ml BSA, and 1.5 - 25 μM of substrate in water. Steady-state kinetics of GlcNAcstatin C were performed in the presence of different concentrations of the inhibitor (0, 35, 70, 140 pM). The reaction mixtures were incubated at 20 °C (RT) for 466 min. For hOGA, 50 μl standard reaction volume contained 2 nM hOGA-GST (53-916), McIlvaine buffer-system (0.2 M Na_2HPO_4 mixed with 0.1 M citric acid) pH 5.7, 0.1 mg/ml BSA, 0-250 μM 4MU-NAG with varying GlcNAcstatin C concentrations (0, 10, 20, 40 nM). The reaction was run for 60 min.

All reactions were stopped (before more than 10 % of the substrate was consumed) by the addition of 100 μl 3 M glycine-NaOH, pH 10.3. The fluorescence of the released 4-methylumbelliferone was quantified using a FLX 800 Microplate Fluorescence Reader (Bio-Tek), with excitation and emission wavelengths of 360 and 460 nm, respectively. The mode of inhibition was visually verified by the Lineweaver-Burk plot (Fig. 1B), and the K_i determined by fitting all fluorescence intensity data to the standard equation for competitive inhibition in GraFit [47] (Table I, II). IC_{50} measurements with a mixture of human hexosaminidase A/B activities (purchased from Sigma, catalogue number A6152) against GlcNAcstatin A-E and PUGNAc were performed using the fluorogenic 4MU-NAG substrate and standard reaction mixtures as described previously

[41, 43] with the following changes: 5 μunits / ml enzyme mixture was used with a fixed substrate concentration at the K_{m} (230 μM) in the presence of different concentrations of the inhibitors, 100 pM to 100 μM (GlcNAcstatins) and 10 pM to mM pM (PUGNAc).

Cell-based assays and Western blots

Cell lines were maintained in DMEM (containing 1 g/l glucose for HEK293, and 4.5 g/l glucose for HeLa, HT-1080, SH-SY5Y and U-2 OS) supplemented with 10% foetal bovine serum. Sub-confluent cells were treated with varying concentrations of inhibitors in the presence of 0.1% DMSO. After 6 hours, cells were washed once in ice-cold PBS and harvested in the following lysis buffer: 50 mM Tris pH 7.4, 0.27 M sucrose, 1 mM Na-orthovanadate, 1 mM EDTA, 1 mM EGTA, 10 mM Na-β-glycerophosphate, 50 mM NaF, 1% Triton-X, 0.1% β-mercaptoethanol, 1 mM benzamidine, 0.1 mM PMSF, 5 μM leupeptin. Cell debris was removed by centrifugation, and supernatants were analysed by immunoblotting. For Western blot analysis, 15-30 μg of total cellular protein were separated by SDS PAGE, and *O*-GlcNAcylation was detected with anti-*O*-GlcNAc antibody CTD110.6. An anti-β-tubulin antiserum was used for loading controls. The *O*-GlcNAc signal in each lane was quantified using the Advanaced Image Data Analyzer software (AIDA) version 3.27, and normalized against the β-tubulin signal.

Results and discussion

GlcNAcstatins - a new family of potent hOGA inhibitors

Exploiting the available structural data of a complex of a *C. perfringens* OGA orthologue (*Cp*OGA, [28, 41]), GlcNAcstatins A-E were designed and synthesized (Fig. 1A, details of synthesis to be reported elsewhere). GlcNAcstatin A-E fall into two subfamilies, based on their modification on the C(2) position of the imidazole ring. GlcNAcstatin A carries the caboxymethyl-group, whereas GlcNAcstatin B-E carry a phenylethyl moiety. GlcNAcstatin C carries an iso-butyl group instead of the smaller *N*-acetyl group in GlcNAcstatin A and B, GlcNAcstatin D an *N*-propionyl group, and GlcNAcstatin E an *N*-imidazole group. The increased length of the *N*-acyl derivative was explored to determine the most useful substituent to specifically inhibit human OGA (hOGA) over the lysosomal hexosaminidases.

GlcNAcstatins are (sub)nanomolar inhibitors of hOGA

A previous report on GlcNAcstatin C showed picomolar inhibiton of an apparent hOGA orthologue from the bacterium *C. perfringens* (*Cp*OGA) [41], whereas inhibition of hOGA remained to be explored. GlcNAcstatin A-E were tested in dose-response experiments against recombinant hOGA, with subsequent Lineweaver-Burk analysis revealing competitive inhibition against the enzymes (Table I, Fig. 1B). GlcNAcstatin A-D inhibit the human enzyme in the low nanomolar to sub-nanomolar range (Table I, Fig. 1B). GlcNAcstatin B and D are the most potent hOGA inhibitors with K_i's of 0.4 and 0.7 nM, respectively, being, to the best of our knowledge, the most potent hOGA inhibitors currently available. GlcNAcstatin A and C are equally potent with K_i's of 4.3 nM and 4.4 nM, respectively. GlcNAcstatin E inhibits only in the μM range.

Tuning of hOGA/hexosaminidase selectivity

All GlcNAcstatin derivatives were evaluated against human lysosomal hexosaminidases to investigate potential selectivity towards hOGA (Table I, Fig. 1C). GlcNAcstatin A is the smallest GlcNAcstatin family member. It carries the *N*-acetyl moiety and the carboxymethyl-group, and inhibits hOGA in the nM range. Assaying lysosomal hexosaminidases HexA/B shows that the compound

equally potently inhibits the GH20 enzymes (K_i of 550 pM) (Table I). The first modification we addressed was to substitute the carboxymethyl group to obtain GlcNAcstatin B, similar to previous work showing that a β-glycosidase from *C. saccharolyticum* is more potently inhibited with a phenylethyl-substituted glucoimidazole [48]. Indeed, GlcNAcstatin B is around 10-fold more potent against hOGA (K_i of 420 pM) than GlcNAcstatin A. However, it also inhibits HexA/B more potently, giving a K_i of 170 pM (Table I). The IC_{50} data show that GlcNAcstatin B is (to our best knowledge) also the most potent HexA/B inhibitor currently known, with a K_i of 170 pM, followed by GlcNAcstatin A (K_i of 550 pM). With these suitably potent inhibitors in hand we attempted to address selectivity by modifying the *N*-acetyl group. The addition of a single methyl group to obtain an *N*-propionyl side chain (GlcNAcstatin D) already leads to different inhibition profiles between human *O*-GlcNAcase and human lysosomal hexosaminidases HexA/HexB (Table I), with a 15-fold reduction in inhibition of HexA/B. Further extension to an isobutyl group (GlcNAcstatin C) reduces HexA/B inhibition more than 200-fold, giving selectivities of 164-fold for hOGA, whereas incorporation of a larger imidazole group resulted in loss of both potency and selectivity (Table I, Fig. 1C).

Probing key GlcNAcstatin binding residues

To further understand the structural basis for selectivity, we determined the crystal structure of *Cp*OGA in complex with GlcNAcstatin D (Fig. 2). These data show that GlcNAcstatin D binds deep into the active site of *Cp*OGA, with the sugar moiety adopting a ^{4}E conformation, and assuming the same conformation as observed for the GlcNAcstatin C complex [41]. Interestingly, the structural data points towards two active site residues that may play a key role in the surprisingly large difference in activity and selectivity of the GlcNAcstatins towards the hOGA/*Cp*OGA and HexA/B. The only non-conserved residue near the *N*-acetyl binding pocket in *Cp*OGA is Val331, corresponding to Cys215 in hOGA. Unbiased $|F_o| - |F_c|$ density of the GlcNAcstatin D complex defines that the *N*-propionyl group points towards this non-conserved Val331 and occupies a single defined conformation, interacting with the $C_{\beta/\gamma}$ carbons (Fig. 2A). Furthermore, the phenyl moiety from GlcNAcstatin D is seen to interact with a solvent-exposed tryptophan (Trp490), similar to the phenyl moiety from PUGNAc and GlcNAcstatin C in the respective *Cp*OGA complexes [28, 41]

(Fig. 2B). From a sequence alignment between *Cp*OGA and hOGA, it is not clear if an equivalently positioned aromatic residue exists in the human enzyme [28]. The relative contributions to binding of these residues were probed by mutagenesis in *Cp*OGA. Mutation of Val331 to cysteine resulted in a mutant enzyme with unaltered steady state kinetics compared to wild type *Cp*OGA (Table II). However, Lineweaver-Burk analysis using GlcNAcstatin C as the inhibitor, gives a 25-fold reduced K_i of 98 pM (Table II) compared to the wild type enzyme. Thus, while the cysteine, conserved in metazoan OGAs, is not involved in catalysis, it does contribute to defining the shape of the *N*-acetyl pocket.

Mutation of Trp490 to alanine resulted in a mutant enzyme that showed a 30-fold reduction in K_m when assayed with the pseudo-substrate 4-methylumbelliferyl-*N*-acetyl-β-D-glucosaminide (Table II). Inhibition by GlcNAcstatin C is similarly affected, with the K_i for W490A-*Cp*OGA being almost 20-fold reduced (K_i = 74 pM versus K_i = 4 pM for the wild type enzyme, Table II). In comparison, PUGNAc exhibits a 3-fold reduced binding affinity against W490A-*Cp*OGA [28]. However, structural comparisons show that the PUGNAc phenylcarbamate moiety occupies a different position in the active site of *Cp*OGA (Fig. 2B) and lacks the stacking interactions with Trp490 that are observed in the GlcNAcstatin complexes. In absence of a hOGA crystal structure, it remains unknown whether an equivalent of Trp490 (His433 in *Bacillus thetaiotaomicron* OGA, [29]) exists in the human enzyme.

GlcNAcstatins effectively induce cellular hyper-O-GlcNAcylation at low nanomolar concentrations

The intended application of the GlcNAcstatins is to inhibit hOGA in live human cells, resulting in hyper-*O*-GlcNAcylation by disrupting the balance between *O*-GlcNAc transfer and hydrolysis. Such modulation of *O*-GlcNAc levels would allow for the study of *O*-GlcNAc-dependent signal transduction processes. To evaluate the use of the GlcNAcstatins for cell biological studies, HEK293 cells were exposed to varying concentrations of GlcNAcstatins for 6 hours, followed by investigation of *O*-GlcNAc levels on cellular proteins by Western blot analysis using an anti-*O*-GlcNAc antibody (CTD110.6) (Fig. 3A). GlcNAcstatin B-D increase cellular *O*-GlcNAc levels of numerous intracellular proteins when used at concentrations as low as 20 nM. GlcNAcstatin A and E appear to be less potent as quantitavely assessed from the Western blots, requiring micromolar

concentrations in the cell-based assay for a marked effect inside the cells. For GlcNAcstatin E, this is in agreement with the *in vitro* inhibition data that show this compound is the weakest hOGA inhibitor (Table I). The reduced cellular activity of GlcNAcstatin A could be due to differences in membrane permeability resulting from the less hydrophobic nature of the C2 carboxymethyl substituent. Together, these results suggest that GlcNAcstatins are cell-permeable compounds that modulate *O*-GlcNAcylation levels within the cells by inhibiting hOGA.

We also have investigated the potency of the most selective GlcNAcstatin (GlcNAcstatin C) against a range of different cell lines (Fig. 3B). HeLa (adenocarcinoma), HT-1080 (fibrosacroma), SH-SY5Y (neuroblastoma) and U-2 OS (osteosarcoma) cells were treated for 6 hours with 20 nM and 5 μM inhibitor concentrations. In comparison to the untreated cells, whole cell lysate analysis with the anti-*O*-GlcNAc-antibody shows a concentration-dependent hyper-*O*-GlcNAcylation in all four cell-lines, with an increase already detectable at 20 nM concentration of the compound (Fig. 3B).

Concluding remarks

We have explored a new family of potent and competitive *O*-GlcNAcase inhibitors, the GlcNAc-statins, based on the GlcNAc-imidazole scaffold. Based on structural analysis with GlcNAcstatin C [41] and GlcNAcstatin D in complex with *Cp*OGA we can explain the potency of this inhibitor family. All GlcNAcstatins interact with the active site of *O*-GlcNAcases forming at least eight conserved hydrogen bonds (Fig. 2A, B), the pyranose ring adopts a favoured ^{4}E conformation and conserved interactions with Asp297 and Asn396 force the N2 substituent to adopt a conformation compatible with the proposed substrate-assisted catalytic mechanism [20, 28, 29], with the carbonyl oxygen approaching the sp^2 hybridised carbon to within 3.4 Å.

GlcNAcstatin A-D inhibit hOGA in the low-nanomolar to sub-nanomolar range, while *Cp*OGA is inhibited in the low picomolar range, implying that there are some (minor) differences in the GlcNAc binding pocket between hOGA and *Cp*OGA, even though the active sites of these enzymes are almost identical as assessed by sequence alignment [28]. We have identified two key active site residues, Val331/Trp490, that are responsible for stronger interactions of GlcNAcstatins with *Cp*OGA compared to hOGA. It still remains unknown to what extent the GlcNAcstatin aglycon can be modified in order to increase the binding affinity for the human active site, given the possible structural divergence between the human/bacterial enzymes in this area.

GlcNAcstatins are to our best knowledge the most potent competitive inhibitors of hOGA. They can be used in cell-based assays in nanomolar concentrations to increase cellular *O*-GlcNAc levels *in vivo* in a range of human cell lines. Thus GlcNAcstatins provide a valuable tool for functional investigations of this post-translational modification and its involvement in signalling pathways within the eukaryotic cell.

Acknowledgements

We thank the European Synchrotron Radiation Facility, Grenoble, for the time at beamline ID14-1. We would like to thank Adel Ibrahim (University of Dundee, Cloning Service, DSTT) for cloning of the hOGA construct and Sharon Shepherd and Mark Dorward for protein expression

and purification. This work was supported by a Wellcome Trust Senior Fellowship and a Lister Institute for Preventive Medicine Research Prize. HCD is supported by the College of Life Sciences Alumni Studentship. The coordinates and structure factors have been deposited with the PDB (PDB entry 2WB5).

References

[1] C. R. Torres, G. W. Hart (1984) Topography and polypeptide distribution of terminal N-acetylglucosamine residues on the surfaces of intact lymphocytes - evidence for *O*-linked GlcNAc. J.Biol.Chem. 259, 3308–3317.

[2] N. E. Zachara, G. W. Hart (2004) *O*-GlcNAc modification: a nutritional sensor that modulates proteasome function. Trends In Cell Biology 14, 218–221.

[3] D. C. Love, J. A. Hanover (2005) The hexosamine signaling pathway: deciphering the "*O*-GlcNAc code". Science STKE 312, 1–14.

[4] G. W. Hart, M. P. Housley, C. Slawson (2007) Cycling of *O*-linked β-*N*-acetylglucosamine on nucleocytoplasmic proteins. Nature 446, 1017–1022.

[5] T. Y. Chou, G. W. Hart (2001) *O*-linked *N*-acetylglucosamine and cancer: messages from the glycosylation of c-Myc. Adv Exp Med Biol 491, 413–418.

[6] K. Liu, A. J. Paterson, R. J. Konrad, A. F. Parlow, S. Jimi, M. Roh, E. J. Chin, J. E. Kudlow (2002) Streptozotocin, an *O*-GlcNAcase inhibitor, blunts insulin and growth hormone secretion. Mol Cell Endocrinol 194 (1-2), 135–146.

[7] A. C. Donadio, C. Lobo, M. Tosina, V. de la Rosa, M. Martin-Rufian, J. A. Campos-Sandoval, J. M. Mates, J. Marquez, F. J. Alonso, J. A. Segura (2008) Antisense glutaminase inhibition modifies the *O*-GlcNAc pattern and flux through the hexosamine pathway in breast cancer cells. J Cell Biochem 103 (3), 800–11.

[8] L. S. Griffith, B. Schmitz (1995) *O*-linked *N*-acetylglucosamine is upregulated in Alzheimer brains. Biochem Biophys Res Commun 213 (2), 424–431.

[9] P. Yao, P. Coleman (1998) Reduction of *O*-linked *N*-acetylglucosamine-modified assembly protein-3 in Alzheimer's disease. Journal of Neuroscience 18 (7), 2399–2411.

[10] K. Liu, A. Paterson, F. Zhang, J. McAndrew, K. Fukuchi, J. Wyss, L. Peng, Y. Hu, J. Kudlow (2004) Accumulation of protein *O*-GlcNAc modification inhibits proteasomes in the brain

and coincides with neuronal apoptosis in brain areas with high *O*-GlcNAc metabolism. J. Neurochem. 89, 1044–1055.

[11] L. Wells, G. W. Hart (2003) *O*-GlcNAc turns twenty: functional implications for post-translational modification of nuclear and cytosolic proteins with a sugar. FEBS Lett. 546, 154–158.

[12] W. Dias, G. Hart (2007) *O*-GlcNAc modification in diabetes and Alzheimer's disease. Mol Biosyst 3, 766–772.

[13] D. A. McClain, W. A. Lubas, R. C. Cooksey, M. Hazel, G. J. Parker, D. C. Love, J. A. Hanover (2002) Altered glycan-dependent signaling induces insulin resistance and hyperleptinemia. Proc. Natl. Acad. Sci. USA 99, 10695–10699.

[14] R. J. Copeland, J. W. Bullen Jr, G. W. Hart (2008) Crosstalk Between GlcNAcylation and Phosphorylation: Roles in Insulin Resistance and Glucose Toxicity. Am. J. Physiol. Endocrinol. Metab. 295, 17–28.

[15] M. S. Macauley, A. K. Bubb, C. Martinez-Fleites, G. J. Davies, D. J. Vocadlo (2008) Elevation of Global *O*-GlcNAc Levels in 3T3-L1 Adipocytes by Selective Inhibition of *O*-GlcNAcase Does Not Induce Insulin Resistance. J Biol Chem 283 (50), 34687–34695.

[16] P. Coutinho, E. Deleury, G. Davies, B. Henrissat (2003) An evolving hierarchical family classification for glycosyltransferases. J. Mol. Biol. 328, 307–317.

[17] B. Henrissat, G. Davies (1997) Structural and sequence-based classification of glycoside hydrolases. Curr. Opin. Struct. Biol. 7, 637–644.

[18] R. Hurtado-Guerrero, H. C. Dorfmueller, D. M. F. van Aalten (2008) Molecular mechanisms of *O*-GlcNAcylation. Curr Opin Struct Biol 18 (5), 551–557.

[19] D. L. Y. Dong, G. W. Hart (1994) Purification and characterization of an *O*-GlcNAc selective *N*-acetyl-β-D-glucosaminidase from rat spleen cytosol. J.Biol.Chem. 269, 19321–19330.

[20] M. S. Macauley, G. E. Whitworth, A. W. Debowski, D. Chin, D. J. Vocadlo (2005) *O*-GlcNAcase uses substrate-assisted catalysis - kinetic analysis and development of highly selective mechanism-inspired inhibitors. J.Biol.Chem. 280, 25313–25322.

[21] M. Horsch, L. Hoesch, A. Vasella, D. M. Rast (1991) *N*-acetylglucosaminono-1,5-lactone oxime and the corresponding (phenylcarbamoyl)oxime - novel and potent inhibitors of β-*N*-acetylglucosaminidase. Eur.J.Biochem. 197, 815–818.

[22] R. S. Haltiwanger, K. Grove, G. A. Philipsberg (1998) Modulation of *O*-linked *N*-acetylglucosamine levels on nuclear and cytoplasmic proteins *in vivo* using the peptide *O*-GlcNAc-β-*N*-acetylglucosaminidase inhibitor *O*-(2-acetamido-2-deoxy-D-glucopyranosylidene)amino-*N*-phenylcarbamate. J.Biol.Chem. 273, 3611–3617.

[23] D. Xing, W. Feng, L. G. Nöt, A. P. Miller, Y. Zhang, Y.-F. Chen, E. Majid-Hassan, J. C. Chatham, S. Oparil (2008) Increased protein *O*-GlcNAc modification inhibits inflammatory and neointimal responses to acute endoluminal arterial injury. Am. J. Physiol. Heart. Circ. Physiol. 295, H335–H342.

[24] N. Lüdemann, A. Clement, V. H. Hans, J. Leschik, C. Behl, R. Brandt (2005) *O*-glycosylation of the tail domain of neurofilament protein M in human neurons and in spinal cord tissue of a rat model of amyotrophic lateral sclerosis (ALS). J. Biol. Chem. 280, 31648–31658.

[25] Y. Akimoto, H. Kawakami, K. Yamamoto, E. Munetomo, T. Hida, H. Hirano (2003) Elevated expression of *O*-GlcNAc-modified proteins and *O*-GlcNAc transferase in corneas of diabetic Goto-Kakizaki rats. Invest Ophthalmol Vis Sci 44 (9), 3802–9.

[26] C. Guinez, A.-M. Mir, V. Dehennaut, R. Cacan, A. Harduin-Lepers, J.-C. Michalski, T. Lefebvre (2008) Protein ubiquitination is modulated by *O*-GlcNAc glycosylation. FASEB J. 22, 2901–2911.

[27] E. J. Kim, B. Amorelli, M. Abdo, C. J. Thomas, D. C. Love, S. Knapp, J. A. Hanover (2007) Distinctive inhibition of *O*-GlcNAcase isoforms by an α-GlcNAc thiolsulfonate. J Am Chem Soc 129 (48), 14854–5.

[28] F. V. Rao, H. C. Dorfmueller, F. Villa, M. Allwood, I. M. Eggleston, D. M. F. van Aalten (2006) Structural insights into the mechanism and inhibition of eukaryotic *O*-GlcNAc hydrolysis. EMBO J. 25, 1569–1578.

[29] R. J. Dennis, E. J. Taylor, M. S. Macauley, K. A. Stubbs, J. P. Turkenburg, S. J. Hart, G. N. Black, D. J. Vocadlo, G. J. Davies (2006) Structure and mechanism of a bacterial β-glucosaminidase having *O*-GlcNAcase activity. Nat.Struct.Mol.Biol. 13, 365–371.

[30] G. Whitworth, M. Macauley, K. Stubbs, R. Dennis, E. Taylor, G. Davies, I. Greig, D. Vocadlo (2007) Analysis of PUGNAc and NAG-thiazoline as Transition State Analogues for Human *O*-GlcNAcase: Mechanistic and Structural Insights into Inhibitor Selectivity and Transition State Poise. J. Am. Chem. Soc. 129, 635–644.

[31] D. J. Mahuran (1999) Biochemical consequences of mutations causing the GM2 gangliosidoses. Biochim Biophys Acta 1455 (2-3), 105–138.

[32] B. L. Mark, D. J. Vocadlo, D. L. Zhao, S. Knapp, S. G. Withers, M. N. G. James (2001) Biochemical and structural assessment of the 1-N-azasugar GalNAc-isofagomine as a potent family 20 β-*N*-acetylhexosaminidase inhibitor. J.Biol.Chem. 276, 42131–42137.

[33] K. A. Stubbs, N. Zhang, D. J. Vocadlo (2006) A divergent synthesis of 2-acyl derivatives of PUGNAc yields selective inhibitors of *O*-GlcNAcase. Org.Biomol.Chem. 4, 839–845.

[34] E. J. Kim, M. Perreira, C. J. Thomas, J. A. Hanover (2006) An *O*-GlcNAcase-specific inhibitor and substrate engineered by the extension of the *N*-acetyl moiety. J.Am.Chem.Soc. 128 (13), 4234–5.

[35] B. Shanmugasundaram, A. Debowski, R. Dennis, G. Davies, D. Vocadlo, A. Vasella (2006) Inhibition of *O*-GlcNAcase by a gluco-configured nagstatin and a PUGNAc-imidazole hybrid inhibitor. Chem. Commun. (Camb.) 42, 4372–4374.

[36] B. L. Mark, D. J. Mahuran, M. M. Cherney, D. Zhao, S. Knapp, M. N. G. James (2003) Crystal structure of human β-hexosaminidase B: understanding the molecular basis of Sandhoff and Tay-Sachs disease. J Mol Biol 327 (5), 1093–109.

[37] M. J. Lemieux, B. L. Mark, M. M. Cherney, S. G. Withers, D. J. Mahuran, M. N. G. James (2006) Crystallographic structure of human β-hexosaminidase A: interpretation of Tay-Sachs mutations and loss of GM2 ganglioside hydrolysis. J. Mol. Biol. 359, 913–929.

[38] S. Yuzwa, M. Macauley, J. Heinonen, X. Shan, R. Dennis, Y. He, G. Whitworth, K. Stubbs, E. McEachern, G. Davies, D. Vocadlo (2008) A potent mechanism-inspired *O*-GlcNAcase inhibitor that blocks phosphorylation of tau *in vivo*. Nat. Chem. Biol. 4, 483–490.

[39] T. Aoyagi, H. Suda, K. Uotani, F. Kojima, T. Aoyama, K. Horiguchi, M. Hamada, T. Takeuchi (1992) Nagstatin, a new inhibitor of *N*-acetyl-β-D-glucosaminidase, produced by *Streptomyces amakusaensis* MG846-fF3. Taxonomy, production, isolation, physico-chemical properties and biological activities. J. Antibiot. 45, 1404–1408.

[40] T. Aoyama, H. Naganawa, H. Suda, K. Uotani, T. Aoyagi, T. Takeuchi (1992) The structure of nagstatin, a new inhibitor of *N*-acetyl-β-D-glucosaminidase. J Antibiot (Tokyo) 45 (9), 1557–8.

[41] H. C. Dorfmueller, V. S. Borodkin, M. Schimpl, S. M. Shepherd, N. A. Shpiro, D. M. F. van Aalten (2006) GlcNAcstatin: a picomolar, selective *O*-GlcNAcase inhibitor that modulates intracellular *O*-GlcNAcylation levels. J. Am. Chem. Soc. 128, 16484–16485.

[42] T. D. Heightman, A. T. Vasella (1999) Recent insights into inhibition, structure, and mechanism of configuration-retaining glycosidases. Angew.Chem.-Int.Edit. 38, 750–770.

[43] S. Pathak, H. C. Dorfmueller, V. S. Borodkin, D. M. F. Van Aalten (2008) Chemical Dissection of the Link between Streptozotocin, *O*-GlcNAc, and Pancreatic Cell Death. Chem. Biol. 15, 799–807.

[44] A. W. Schuettelkopf, D. M. F. van Aalten (2004) PRODRG: a tool for high-throughput crystallography of protein-ligand complexes. Acta Cryst. D60, 1355–1363.

[45] P. Emsley, K. Cowtan (2004) Coot: model-building tools for molecular graphics. Acta Cryst. D60, 2126–2132.

[46] G. N. Murshudov, A. A. Vagin, E. J. Dodson (1997) Refinement of macromolecular structures by the maximum-likelihood method. Acta Cryst. D53, 240–255.

[47] R. J. Leatherbarrow (2001) GraFit. Version 5, Erithacus Software Ltd., Horley, U.K.

[48] N. Panday, Y. Canac, A. Vasella (2000) Very strong inhibition of glucosidases by C(2)-substituted tetrahydroimidazopyridines. Helv.Chim.Acta 83, 58–79.

Figure legends

1. A) Chemical structures of the glycosidase inhibitors PUGNAc, nagstatin and the GlcNAc-statin scaffold.

   B) Lineweaver-Burk analysis of hOGA steady-state kinetics measured in presence of 0-40 nM GlcNAcstatin C. Data were fitted using the standard equation for competitive inhibition in the GraFit program [47].

   C) Dose-response curve of GlcNAcstatin A-E incubated with lysosomal hexosaminidases HexA/HexB. Data were fitted using the standard IC_{50} equation in the GraFit program [47].

2. A) Stereo figure of GlcNAcstatin D (sticks with green carbon, red oxygen, blue nitrogen atoms) in the active site of *Cp*OGA (sticks with grey carbon). Hydrogen bonds are indicated by black dashed lines. Unbiased $|F_o| - |F_c|$, ϕ_{calc} electron density map (2.75 σ) is shown as cyan chickenwire.

   B) Stereo view of superimposed crystallographically determined complexes of *Cp*OGA with GlcNAcstatin C (2J62.pdb) (colour scheme as in panel A) and PUGNAc (2CBJ.pdb) (sticks with light blue carbon), black dashed lines showing hydrogen bonds for *Cp*OGA-GlcNAcstatin complex.

3. Immunoblot detection of *O*-GlcNAc modifications on cellular proteins using an anti-*O*-GlcNAc antibody. The increase in *O*-GlcNAc levels in comparison to untreated samples is depicted in the bar-diagram underneath the blot.

   A) HEK293 cells were treated with GlcNAcstatin A-E for 6 hours with the indicated concentrations.

   B) GlcNAcstatin C was added to HeLa, HT-1080, SH-SY5Y, U-2 OS cells for 6 hours with the identical inhibitor concentrations as in panel A.

Table I

Inhibition data of GlcNAcstatin A-E and PUGNAc against lysosomal hexosaminidases HexA/HexB, hOGA and the compounds selectivity for hOGA.

Compound	HeX A/B K_i [nM] (1)	hOGA K_i [nM]	Selectivity (GH20/hOGA)
GlcNAcstatin A	0.55 ± 0.05	4.3 ± 0.2	n.s.
GlcNAcstatin B	0.17 ± 0.05	0.42 ± 0.06	n.s.
GlcNAcstatin C	550 ± 10	4.4 ± 0.1	164
GlcNAcstatin D	2.7 ± 0.4	0.74 ± 0.09	4
GlcNAcstatin E	1100 ± 100	8500 ± 300	n.s.
PUGNAc	25 ± 2.5	35 ± 6 (1)	n.s.

n.s. = no selectivity for hOGA.

(1) = the Cheng-Prusoff equation ($K_i = IC_{50}/1+([S]/K_m)$) was used to convert the IC_{50} values to an absolute inhibition constant (K_i).

Table II

Michaelis-Menten parameters of *Cp*OGA wild type and mutants and K_i's against GlcNAcstatin C.

enzyme	K_i [nM]	K_m [μM]	k_{cat} [s^{-1}]
WT	4.6 ± 0.1	2.9 ± 0.2	10.5 ± 0.2
V331C	98.1 ± 6.4	6.8 ± 0.4	17.3 ± 0.7
W490A	74.0 ± 5.6	100 ± 10	65 ± 3

Biochemical Journal Immediate Publication. Published on 10 Mar 2009 as manuscript BJ20090110

Figure 1

A)

PUGNAc

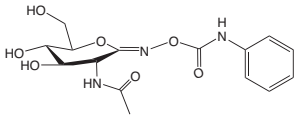

Nagstatin

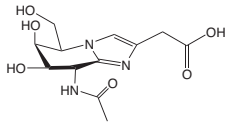

GlcNAcstatin A-E

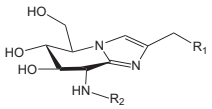

	R_1	R_2
A:	$CHOCH_3$	$COCH_3$
B:	CH_2-Phenyl	$COCH_3$
C:	CH_2-Phenyl	$COCH(CH_3)_2$
D:	CH_2-Phenyl	$COCH_2CH_3$
E:	CH_2-Phenyl	Imidazole

B)

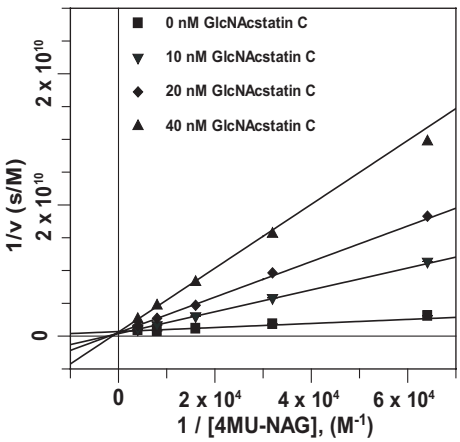

C)

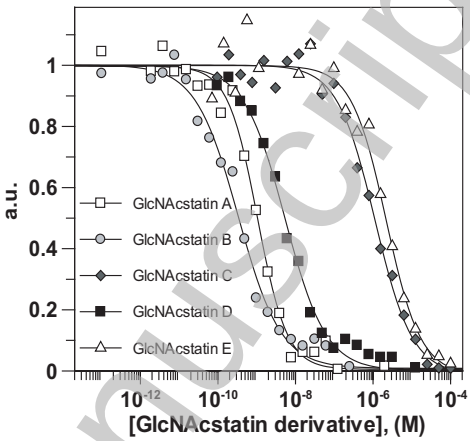

Biochemical Journal Immediate Publication. Published on 10 Mar 2009 as manuscript BJ20090110

Figure 2

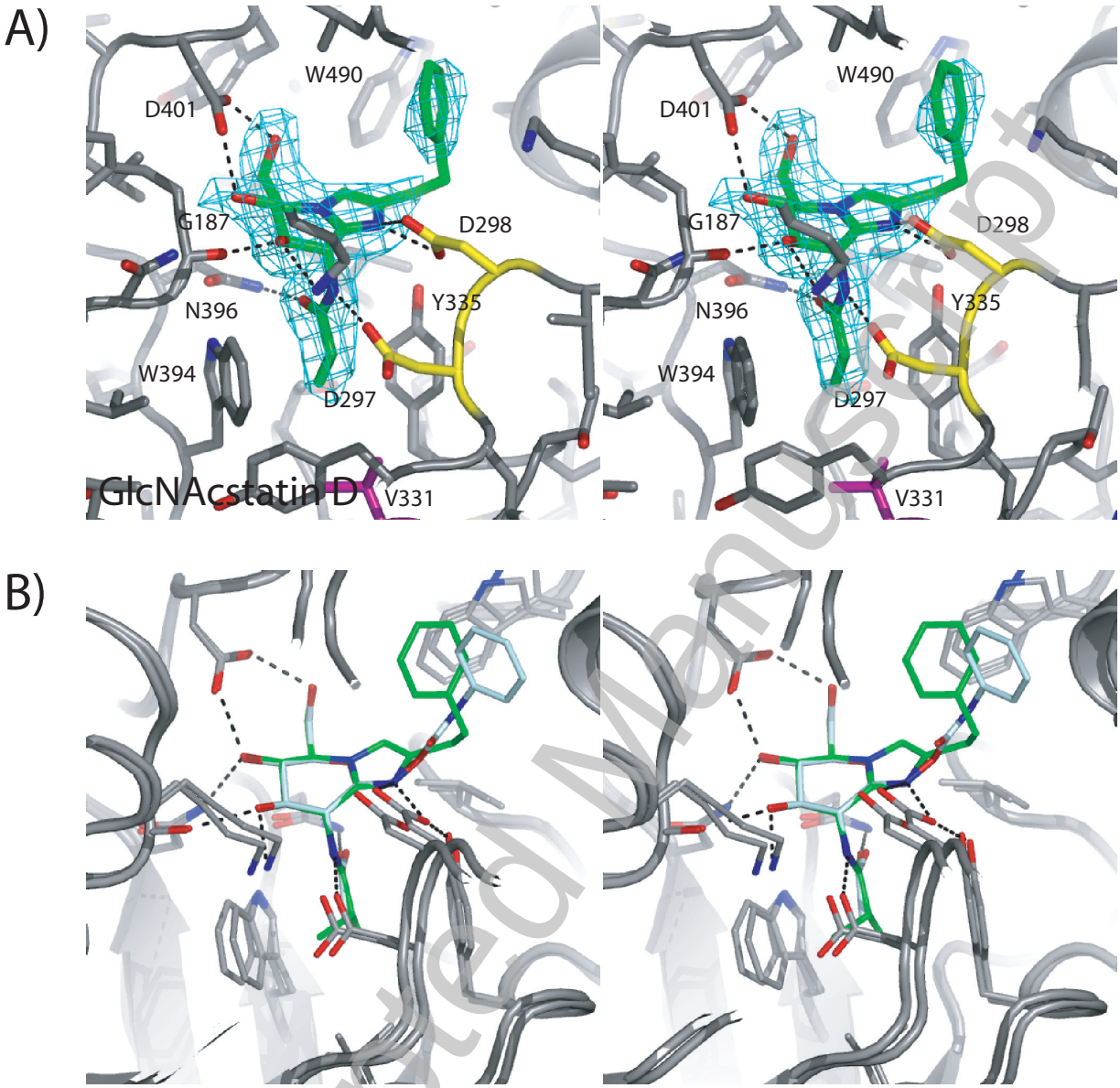

Biochemical Journal Immediate Publication. Published on 10 Mar 2009 as manuscript BJ20090110

Figure 3